Journal of
GEOPHYSICAL RESEARCH

VOLUME 73 JANUARY 1, 1968 No. 1

Magnetospheric Properties Deduced from OGO 1 Observations of Ducted and Nonducted Whistlers

R. L. SMITH AND J. J. ANGERAMI[1]

Radioscience Laboratory
Stanford University, Stanford, California 94305

The OGO 1 satellite has yielded evidence for both ducted and nonducted modes of whistler propagation in the magnetosphere. Two new types of nonducted whistlers have been identified: the 'magnetospherically reflected' whistler and the 'Nu' whistler. These whistlers have never been observed on the ground. Their unique properties result in part from the presence of ions that permit reflection of whistler-mode energy in the magnetosphere. These phenomena provide a new tool for study of the distribution of ionization in the magnetosphere. Ducted whistlers from OGO 1 have provided the first in situ observations of whistler ducts. Near $L = 3$, the equatorial separations between ducts ranged from 50 to 500 km, and the equatorial thicknesses were about 400 km. The analysis yielded independent experimental support for the diffusive equilibrium model of distribution of ionization along the field lines in the plasmasphere. Some evidence was found of distortion of the magnetic field on the nightside at $L \sim 3$, possibly due to oblique incidence of the solar wind on the earth's field.

1. INTRODUCTION

Many natural VLF whistler and noise phenomena are observable in satellites but not on the ground because of refraction or reflection of the downcoming waves in the ionosphere and magnetosphere. Whistlers that reach the ground are interpreted as having propagated in field-aligned ducts of enhanced ionization. Within such ducts, the wave normals are constrained to lie within a small cone of angles around the direction of the magnetic field [*Smith*, 1961]. Some of these wave normals are in a favorable direction to allow the downcoming energy to cross the lower boundary of the ionosphere [*Helliwell*, 1965]. In a 'smooth' magnetosphere without ducts, whistler energy propagates in the so-called 'nonducted' mode and is guided only to a limited extent along the magnetic field, in the manner originally described by *Storey* [1953]. In this case, calculations show that the angle between the wave normal and the geomagnetic field tends to become large [*Yabroff*, 1961], so that the energy cannot propagate across the lower boundary of the ionosphere. Furthermore, the effect of ions can cause downcoming waves to be reflected inside the magnetosphere before reaching ionospheric heights [*Kimura*, 1966].

Rocket and satellite experiments have corroborated the fundamental difference between ground and ionospheric observations in the VLF range through evidence of relatively higher levels of activity at ionospheric heights and the presence in the ionosphere of a number of types of whistlers not seen on the ground [e.g., *Barrington and Belrose*, 1963; *Cartwright*, 1964*a*, *b*; *Brice and Smith*, 1965]. A high-altitude satellite such as OGO 1 provides a unique platform for whistler research, since the receiver traverses regions in which the whistler rate is sufficiently large and the dispersion properties

[1] On leave from Escola Politécnica da Universidade de São Paulo, Brazil.

of the events sufficiently developed to enable clear identification and detailed study of both ducted and nonducted events. (Initially the OGO 1 perigee and apogee were 280- and 149,400 km altitude, the inclination 31°, and the period approximately 64 hours.) Thanks to the long and successful lifetime of OGO 1, the Stanford University/Stanford Research Institute VLF experiment onboard has led to the discovery of a number of new VLF phenomena, the verification of several important predictions of VLF propagation theory, and the extension of knowledge of certain features of the magnetosphere such as ducts and the distribution of ionization along the field lines. These results are partially summarized in the present paper through description of the dispersive properties of whistlers received at altitudes of 6,000–12,000 km and magnetic latitudes of 15–30°, a region previously unexplored by vehicles carrying VLF receivers.

The following sections deal with three major subject areas: (1) nonducted propagation, (2) ducted propagation, and (3) properties of the magnetosphere deduced from ducted whistlers. The material on nonducted propagation is primarily devoted to a new phenomenon, the 'magnetospherically reflected' or MR whistler.

2. Description of the Experiment

The Stanford University/Stanford Research Institute VLF experiment on OGO 1 [see *Rorden et al.*, 1966] uses a single turn magnetic loop antenna (a torus) with a 3-meter diameter and a torus diameter of 7.5 cm. The signals are fed in parallel into 3 stepping receivers covering the 0.3–100 khz range and into one broadband (0.3–12.5 khz) receiver. The latter provides the data used in this paper. The signals in the broadband receiver are log-compressed from 80 db to a 20 db dynamic range and used to frequency modulate a 400-Mhz carrier. (The log compressor has an instantaneous AGC action such that a very strong signal may suppress a weaker one.) The information is then telemetered to the ground in real time through the special purpose telemetry channel, thus providing high time resolution in the entire band 0.3–12.5 khz.

3. Associated Ground Measurements

Detailed analysis of whistlers received aboard satellites requires knowledge of the time of the causative lightning impulse. This can be identified through VLF broadband recordings at ground stations located within several hundred kilometers of the foot of the field line passing through the satellite. The identification of the source is made by comparisons of several similar events in the satellite and ground data; precise timing is therefore needed in connection with both sets of data. Such timing can be obtained from local clocks, or better, from transmissions of VLF stations.

The present study employed data collected by the telemetry stations and VLF ground recording stations listed in Table 1. Also listed are the VLF transmitters used for timing.

4. OGO 1 Studies of Nonducted Propagation

The MR whistler; introduction. The major new phenomenon to be reported here is the magnetospherically reflected or MR whistler. A frequency-time spectrum of such a whistler is shown in Figure 1 (see page 15, photographic section near end of this article). The MR whistler usually consists of a series of traces, each exhibiting a frequency of minimum travel time or nose frequency. The nose frequency decreases with increasing trace number and has a value lower than the expected nose frequency of ducted whistlers by factors of from 3 to 10 or more. Successive traces of the MR whistler frequently occur in closely spaced pairs. Because the general appearance of the successive traces suggests an echoing phenomenon, John Katsufrakis of our laboratory suggested that the propagation shown by the ray paths calculated by *Kimura* [1966] could explain the observations.

Because simultaneous ground records were not available for the event in Figure 1, the exact time of origin of the causative atmospheric could not be determined. An approximate origin, indicated by an arrow in the figure, was determined by fitting to the first whistler component an 'Eckersley's law' overlay of $t = Df^{-1/2}$, where t is travel time, f is frequency, and D is a constant. This equation is, however, not exact for nonducted whistlers, even for the lower frequencies.

Background of the MR whistler study. Kimura [1966] anticipated the MR phenomenon through calculations of ray paths in a smooth magnetosphere (without field aligned irregulari-

TABLE 1. Telemetry and VLF Ground-Recording Stations

Symbol	Location	Geographic Latitude	Geographic Longitude
	Telemetry Stations for OGO 1		
ROS	Rosman, North Carolina	35°N	83°W
ST	Stanford, California	37°N	122°W
JO	Johannesburg, South Africa	26°S	26°E
	VLF Receiving Stations		
BY	Byrd Station, Antarctica	80°S	120°W
EI	Eights Station, Antarctica	75°S	77°W
ELT	USNS ELTANIN	61°S	101°W
GW	Great Whale River, Canada	55°N	80°W
SES	Suffield Experimental Station, Alberta, Canada	50°N	111°W
ST	Stanford, California	37°N	122°W
	VLF Transmitters		
MBA (18 khz)	Summit, Canal Zone	9°N	80°W
NPG (18.6 khz)	Jim Creek, Washington	48°N	122°W
OMEGA (10.2 khz)	Haiku, Hawaii	21°S	156°W

ties) in which the presence of both electrons and ions was considered. One of his calculated ray paths, illustrated in Figure 2, shows regions where the rays turn around quite abruptly and undergo what may be called a 'magnetospheric reflection.' Kimura made a preliminary calculation of the attenuation at the turning points and concluded that waves associated with the kind of ray path indicated in Figure 2 might be observed by a satellite-borne receiver.

The phenomenon of a magnetospheric reflection involves the lower hybrid resonance (LHR). The LHR frequency defines a critical frequency below which propagation is possible at all wave normal angles (i.e., the refractive index surface is closed), and above which propagation is possible only within a certain cone of angles about the direction of the static field [*Smith and Brice,* 1964]. The LHR frequency is a function of the magnetic field strength and the density of ions and electrons. Except for some special regions at altitudes below about 1000 km, the LHR frequency decreases with increasing altitude.

Reflection in the magnetosphere may be described as follows: as a nonducted whistler propagates roughly along the magnetic field lines, the wave normal angle of the whistler wave does not rotate as fast as the geomagnetic field. In other words, the wave normal lags behind the static field, tending toward 90° with respect to the latter. As long as the frequency of the whistler is above the local lower hybrid resonance frequency, the open nature of the refractive index surface prevents the wave normal from passing through 90°. As the energy at a given frequency moves toward the earth, the LHR frequency increases until it is greater than the whistler frequency, allowing transverse propagation. The waves may then refract through the region of transverse propagation and reverse the direction of the ray. The reflection process is properly a refraction, but since this occurs in a region much smaller than the rest of the ray path, it is convenient to use the word 'reflection.'

Previous satellite data on a kind of magnetospheric reflection were obtained for the 'subprotonospheric' or 'SP' whistler [*Carpenter et al.,* 1964]. This whistler, which appears to echo back and forth between the lower ionosphere or ground and an upper region at about 1000 km, was interpreted as involving a refraction of the upgoing wave normal through 90° (near 1000 km) and a consequent reversal of the ray direction [*Smith,* 1964]. Beyond this similarity in the nature of the 'reflection,' the SP and MR events differ markedly, in that they involve

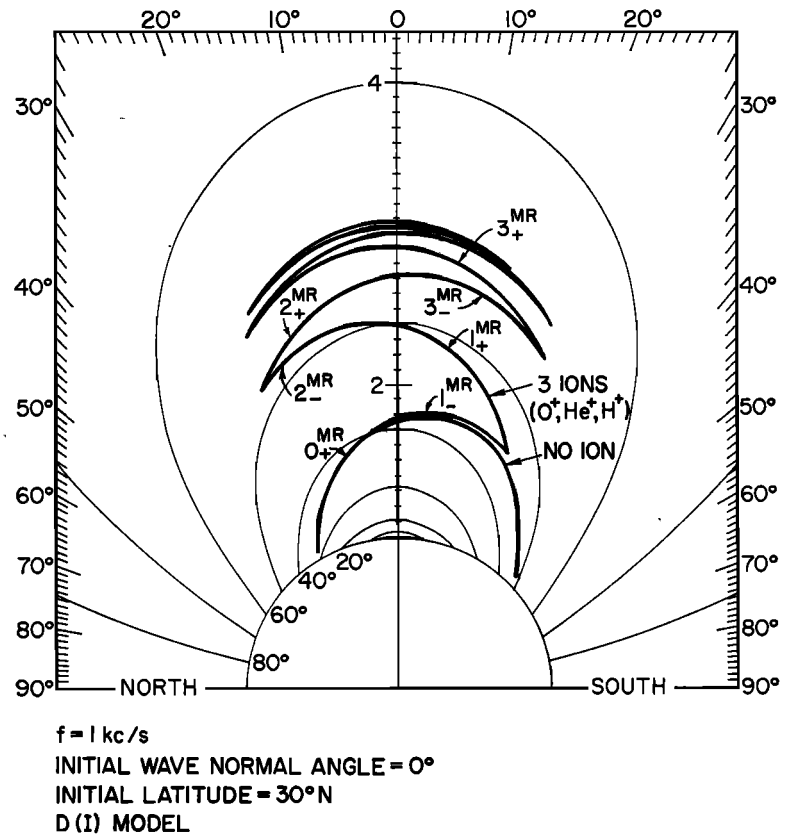

Fig. 2. Ray tracing for nonducted whistlers. In a smooth magnetosphere the effect of ions produces reflection of the ray at some point in the magnetosphere where the lower hybrid resonance frequency is higher than the wave frequency. The whistlers produced by propagation in this mode are thus termed 'magnetospherically reflected.' The $D(I)$ ion density model used in this ray tracing is a diffusive equilibrium model discussed in a paper by *Kimura* [1966], where this figure has appeared. The various portions of the ray path are identified by hop numbers that have been added to the original figure (cf. Figures 1 and 4).

different regions of space, path lengths, and processes by which large wave normal angles develop.

Before presenting details of the MR observations, it is necessary to develop a nomenclature for use in describing the various whistler components. This is done in the following paragraphs.

Terminology for describing whistlers observed in space. A (ducted) whistler observed on the ground has completed an integral number of traverses of the magnetosphere. One that makes a single traverse is called a one-hop whistler; one that reflects and returns to the hemisphere of origin is called a two-hop whistler. This terminology will first be extended to satellite observations of ducted whistlers as shown in Figure 3. The magnetic equator is used as an additional division. A whistler that propagates to the satellites without crossing the magnetic equator is called a 0_+ whistler (or occasionally, a short fractional hop whistler). One that has crossed the magnetic equator but which has not suffered a reflection is termed a 1_- whistler. The packet of energy that produces the 1_- event may also be reflected at ionospheric heights (or possibly at the ground) and again reach the satellite, producing a 1_+ whistler. A satellite in the southern hemisphere, observing signals resulting from a northern hemisphere lightning flash, might observe a 1_- whistler, then a 1_+ whistler, etc., as shown in Figure 3*b*. Observa-

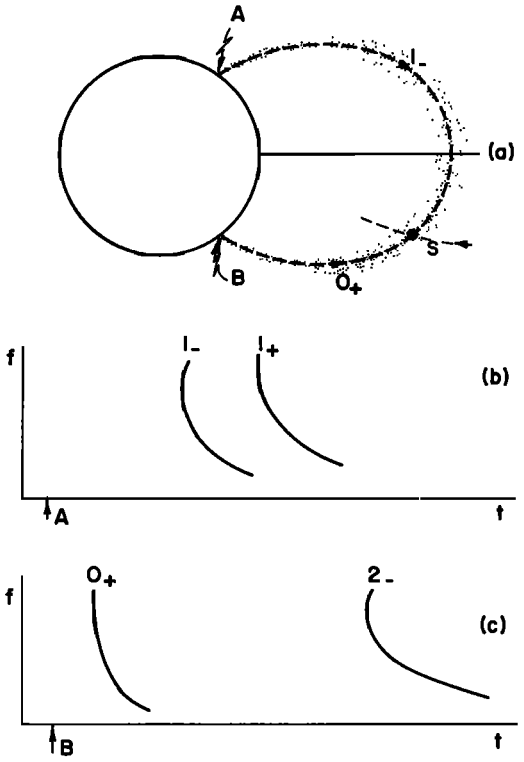

Fig. 3. (*a*) The dashed line represents the center of a field-aligned duct of enhanced ionization able to trap electromagnetic waves in the whistler mode. (The thin broken line is a sketch of the portion of the OGO 1 orbit corresponding to the ducted whistlers of October 20, 1964). Lightning at *A* and *B* may produce whistlers whose frequency-time spectra observed at the satellite *S* are sketched in (*b*) and (*c*), respectively.

tions in the southern hemisphere from a source in the southern hemisphere would yield a 0_+ whistler, then a 2_- whistler, etc., as shown in Figure 3*c*.

This nomenclature may conveniently be extended to nonducted whistlers through reference to Kimura's ray tracing shown in Figure 2. The ray between the hemisphere of origin and the equator is classified as 0_+^{MR}, the ray between the equator and the first magnetospheric reflection 1_-^{MR}, the ray between the first magnetospheric reflection and the equator 1_+^{MR}, and so on. The superscript MR indicates that the energy has been or will be magnetospherically reflected. Regions on the ray paths are so labeled in the figure.

Propagation paths of MR whistlers to a satellite. The ray path in Figure 2 shows the result of excitation of a single frequency at one initial latitude. A lightning source can excite whistler-mode signals in the ionosphere to distances of a few thousand kilometers. Thus a range of ray paths similar to the one in Figure 2 can be excited by one source. A discrete number of these rays may intersect a satellite in the magnetosphere. As an illustration, three such ray paths excited by a single lightning source are sketched in Figure 4*a* for a particular frequency *f*. The satellite *S* is shown in the hemisphere opposite to the lightning source. Energy at different frequencies, propagating in paths topologically similar to path *A*, results in the 1_-^{MR} whistler whose frequency-time spectrum is shown by *A* in Figure 4*b*. Similarly, energy reflected in the magnetosphere in paths topologically similar to *B* and *C* result in the 1_+^{MR} and 3_-^{MR} whistlers labeled *B* and *C*. Note that the travel time difference between components *A* and *B* is less than that between *B* and *C*. This pairing of components can be understood in terms of the ray path lengths of Figure 4*a*.

Similar ray paths and corresponding whistlers are sketched in Figures 4*c* and *d*, except that the satellite *S* is now in the same hemisphere as the source. Component *B'* (now a 2_-^{MR} whistler) is seen to be closer to *C'* (2_+^{MR}) than to *A'* (0_+^{MR}). Again the pairing of traces can be understood in terms of the ray path lengths shown in Figure 4*c*. One would expect nearly equal spacing between the traces if the satellite were at the equator.

Experimental confirmation of the MR whistler concept. The consistency between MR whistler observation and the kind of ray path illustrated in Figures 2 and 4 is demonstrated in the sequence of observations in Figure 5 (see page 15). In this sequence, the satellite moves from a dipole latitude of 9.9°S to 6.8°N. The satellite position and ray paths corresponding to the observations of Figures 5*a* and 5*f* are sketched in Figures 4*a* and 4*c*, respectively.

The approximate times of occurrence of the causative atmospherics are shown by arrows in Figure 5 and were determined from an overlay technique as discussed earlier. It is inferred that the lightning sources for the whistlers shown were located in the northern hemisphere, since the dispersion of the leading trace is reduced as the satellite progresses northward.

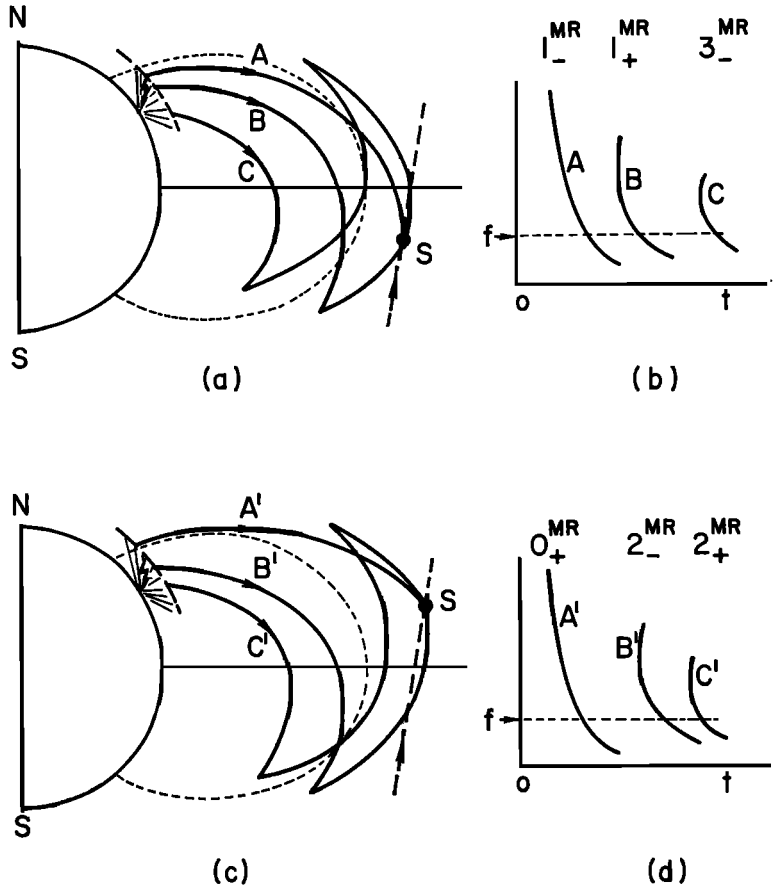

Fig. 4. Sketches of ray tracings for a fixed frequency in a smooth magnetosphere and corresponding spectra of MR whistlers received on satellite S. For reference, a thin broken line indicates a dipole field line. (The thick broken line is a sketch of the portion of the OGO 1 orbit corresponding to the observations of Figure 5.) In (*a*) the satellite is south of the magnetic equator, and path *C* is much longer than path *B*. Accordingly, in (*b*), the spectra of traces *A* and *B* are more closely paired. In (*c*) the satellite is shown north of the magnetic equator, and paths *B'* and *C'* have less difference. Accordingly in (*d*) the spectra of components *B'* and *C'* are more closely paired. The starting latitude at ionospheric heights varies with satellite position, trace number (as schematically indicated), and frequency.

Note the way the traces tend to occur in pairs, and further, the way in which the pairing is a function of latitude. This variation is just what one would expect from the discussion in the previous section (Figure 4). When the satellite is in the opposite hemisphere from the source, the second (1_+^{MR}) trace is closer in time to the first (1_-^{MR}) trace than the third (3_-^{MR}) trace (Figure 5*a*). Near the equator (Figure 5*d*), the traces show nearly equal separation. When the satellite is in the same hemisphere as the source, the pairing of traces is reversed, so that the second trace is now closer to the third trace than to the first trace (Figure 5*f*).

The peculiar frequency-versus-time properties of the MR whistler present challenging problems in interpretation. A full description of the ray path behavior of the MR whistler is complicated, since for a given observation point the initial latitude of each ray is a function of frequency and hop number. Bruce Edgar of our laboratory has carried out a series of ray tracings from which it has been possible to explain in considerable detail the major features of the

MR whistlers. Preliminary results have been reported [*Edgar and Smith*, 1966], and a more complete report based on this work is now in preparation.

Examples of the Nu whistler, a version of the MR whistler. A case study of nonducted whistlers is shown in Figure 6. In this sequence the satellite geomagnetic latitude varies from 27.2 to 30.8°N, the L shell from 2.44 to 2.90, and the altitude from 6000 to 7200 km. Simultaneous ground-station VLF records were available in both hemispheres from Suffield Experimental Station, Canada (SES), and Bryd Station, Antarctica (BY). The causative atmospherics could be identified for nearly all of the whistlers, one of the relevant ground records being shown in panel (*a*). The times of occurrence of the causative atmospherics for most of the whistlers of panels (*b*)–(*f*) are indicated by arrows below the records. Northern hemisphere sources are marked (SES) and southern hemisphere sources (BY), according to the ground recording on which the source was identified (see Table 1). The relations between the sources and the corresponding whistler traces are shown above each record by dashed lines and identification symbols. A superscript MR identifies a magnetospherically reflected whistler trace. Some of the 2_- or 2_+ whistlers do not have superscripts, indicating that the whistler was ducted over at least part of the propagation path.

The data sequence of Figure 6 was chosen because: (1) it demonstrates MR whistlers caused by sources in both hemispheres, clearly identified in each case; (2) it demonstrates the development of a special form of the MR whistler called the 'Nu' whistler; and (3) it shows a spectacular form of emission or noise triggered by an MR whistler (panel (*f*)).

Panels (*a*) and (*b*) are aligned for the same time period to show a ground and satellite comparison. In panel (*b*) the 0_+ whistler is followed by two MR components (2_-^{MR} and 2_+^{MR}), and a 2_+ whistler that is probably ducted over most of its path. The latter may possibly contain a 2_- component. In this record the 0_+ whistler (possibly nonducted) is fairly strong and only the higher frequencies in the MR components are seen. These upper frequencies show a diffuse character and some evidence of emissions, both common features of the MR event. As the satellite progresses to higher L values, the travel time of the MR components increases. In the sequence from panels (*b*) to (*e*) there is a tendency toward weaker 0_+ components and enhanced MR components at low frequencies. In panels (*d*) and (*e*) the 0_+ whistler is missing, but the 2_-^{MR} and 2_+^{MR} and even the 4_-^{MR} and 4_+^{MR} traces are present. This behavior is consistent with an equatorward shift in the position of the lightning source. Preliminary ray tracing results have shown that the impulsive energy entering the ionosphere at low latitudes excites mainly the lower frequencies of the higher-order components, whereas the energy entering the ionosphere at higher latitudes excites mainly the first trace and the higher frequencies of the higher-order components.

The whistlers in panel (*e*) join at their lowest frequency, and are called 'Nu' whistlers. The sequence of Figure 6 therefore shows that the Nu whistler is just a special case of the MR whistler. The energy at frequencies below the 'joining' frequency is not observed, presumably because it is reflected above the position of the satellite. Energy at frequencies above the joining frequency is reflected below the point of observation, and hence two traces are seen. Since the reflection is only possible at frequencies below the lower hybrid resonance, it is concluded that the LHR frequency at the satellite is somewhat greater than the frequency at which the two traces join.

Panel (*f*) of Figure 6 shows a strong whistler in which the two-hop MR components excite an emission that endures for many seconds. The emission mechanism is not known, but there are features of MR whistlers that make interaction with particles likely. The waves travel very near the resonance cone and have a very large refractive index. Furthermore, the waves have a large electric vector in the wave normal direction (nearly perpendicular to the magnetic field direction).

Also shown in panel (*f*) is a whistler component identified as 2_+. A similar trace is seen in panel (*b*). The dispersion of this component does not change as rapidly with time as that of the other components. A tentative explanation of this whistler is that it is basically a two-hop 'ducted' whistler propagating at an L value less than that of the satellite. Upon reflection at the

ionosphere, part of the energy leaves the duct and propagates to the satellite in the nonducted mode.

Other nonducted events. Figure 7 shows some unexplained phenomena associated with MR whistlers. The records were taken during an inbound pass on March 18, 1965, between 1724 and 1930 LMT, in the range $L = 2.68$ to $L = 2.27$. Letters replace the regular symbolism when the exact nature of the trace is not known.

Panel (*a*) shows an atmospheric source identified on a ground record from Great Whale (Canada) that resulted in a 1_- ducted whistler in the satellite. This is followed by two rising tones labeled *A* and *B* and finally by a more or less constant tone near 3 khz, *C*. Trace *A* is possibly a 1_-^{MR} whistler, but with a great deal of frequency and amplitude modulation on the signals. Trace *B* may be a 1_+^{MR} whistler. Note the sharp upper frequency cutoff of this component. Trace *C* is a related event that has a very sharp low-frequency cutoff. This trace may be a three-hop MR whistler. Notice the general increase of noise following these traces. In panel (*b*) the simple 1_- ducted whistler is seen again. Trace *A* is much more disturbed than the corresponding trace in panel (*a*). A portion of trace *B* is also evident and again exhibits a sharp cutoff. Only a small portion of the low-frequency cutoff of trace *C* is evident, but the noise after these traces is seen quite well.

Panel (*c*) shows some MR traces caused by lightning sources identified at Great Whale River. These have some peculiar extra structure associated with them. The whistler resulting from the second (GW) source shows first a set of fairly normal Nu whistler traces that join at a frequency of approximately 2 khz. These traces are similar to many other traces seen earlier in this run. Superimposed on this structure are two higher-frequency descending tones similar to those following the 1_- ducted trace in panel (*b*). These additional traces join onto the two rising tones of the normal Nu whistler at a frequency of about 6 khz. The appearance is that of two additional Nu whistlers coupled onto the more or less well-behaved Nu whistler with the 2-khz joining frequency. In the case of the whistler resulting from the first source in panel (*c*), only the unusual high-frequency Nu whistlers are observed.

The presence of a number of ducted traces at $t \sim 1$–2 sec on the records of panel (*c*) indicates the presence of field-aligned ducts, possibly at lower *L* shells. One speculative explanation of some of the unusual traces in panels (*a*), (*b*), and (*c*) is that large-scale irregularities or ducts may support a number of modes by which the energy can reach the satellite.

Panels (*d*) and (*e*) of Figure 7 contain another set of unexplained traces, these having originated in atmospherics identified on the records of Eights Station. The 0_+ components are first observed, and then a set of traces labeled *E* and *F* appear. These traces are apparently Nu whistlers. There is evidence that both sets of Nu whistlers are in the two-hop category, suggesting multiple paths, possibly due to large-scale irregularities in the magnetosphere. Another interesting feature, particularly of the *F* traces, is a tendency for the frequency of the traces to rise in a step-wise fashion. This is again suggestive of a peculiar mode structure of propagation. The frequency of the discontinuity is nearly the same as the minimum frequency of the 'unusual' Nu whistler traces in panel (*c*) (~6 khz). Also shown in panel (*e*) is a source at Great Whale that causes a 1_-^{MR} and 1_+^{MR} whistler. The phenomena shown in Figure 7 are not well understood and offer possibilities for further research.

5. OGO 1 Studies of Ducted Propagation

Expected nature of the observations. Whistlers received on the ground have been interpreted as resulting from propagation along ducts of field-aligned enhancements of ionization [*Smith*, 1961]. Based on the ground observations, several features of ducted whistlers observed in the magnetosphere above a few thousand kilometers may be predicted:

(1) The frequency-time spectra of ducted whistlers should agree closely with those predicted by the strictly longitudinal approximation, as in the case of whistlers received on the ground.

(2) The ratio of travel times of fractional hop components excited by sources in opposite hemispheres (0_+ and 1_-, Figure 3) should be in close agreement with calculated ratio using the longitudinal approximation and a unique path.

(3) When several components are observed at a given point, their travel times should be

simply interrelated over a wide range of frequencies. This property indicates a unique path and has its parallel in ground observations of echoing of whistlers along a single duct.

(4) The shape of the spectrum should change more or less discretely with satellite position, in a manner consistent with the traversal of a series of separate ducts.

The above properties may not be exhibited by whistlers observed on satellites at ionospheric heights. For instance, both the Alouette 1 and the POGO satellites sometime receive trains of whistlers with components at different nose frequencies. These separate components are probably ducted over most of their paths, propagating along different L shells. The energy reaches the satellite either by leakage from the duct below altitudes of a few thousand kilometers or by internal reflection at the lower boundary of the ionosphere.

Details of the observations. The best examples of ducted whistlers observed so far on OGO 1 were recorded at the Stanford telemetry station during the inbound pass of October 20, 1964, between 0921 UT and 0933 UT. In this 12-minute interval the geomagnetic coordinates of the satellite changed from $L \sim 3.4$, 16.0°S, to $L \sim 2.9$, 19.2°S. The local time at the satellite was about 2300. VLF ground records were available for the entire period of interest. Examples of simultaneous ground and satellite data from this pass are shown in Figures 8 and 9, with the satellite records on the middle panels. VLF ground signals from a narrow band centered at 18.0 khz (recorded in a different channel of the same magnetic tape) have been injected at the bottom of the records. The dashes are second marks from the station NBA, Panama. The geomagnetic coordinates of the satellite were $L \cong 3.2$, $\delta \cong 17.4$°S for Figure 8, and $L \cong 3.1$, $\delta \cong 17.6$°S for Figure 9, these positions being approximately those shown schematically in Figure 3*a*. δ is the central angle between the satellite position and the point of minimum magnetic field intensity on the line of force passing through the satellite, as determined with the *Jensen and Cain* [1962] coefficients.

The OGO 1 record of Figure 8*b* exhibits several 1_- whistlers. Three of these are so labeled, and the corresponding causative lightning impulses (identified on the basis of consistency) are indicated on the SES (top) record by horizontal dashed lines and arrows. The sources for the other 1_- components on panel (*b*) can easily be found by comparison of travel times. The lightning sources seen in the SES record were also detected at Stanford by the narrowband receiver at 18.0 khz, and appear on the middle record as dots near zero frequency. The lightning source at ~3.6 sec, which causes a well-defined 1_- whistler, also produces two-hop whistlers observed at SES. Figure 3*a* shows a schematic diagram of the path of the 1_- whistler.

Panel (*c*) in Figures 8 and 9 exhibits records made in the South Pacific Ocean aboard the USNS Eltanin. The propagation delay from the NPG transmitter to the Eltanin (~40 msec) was taken into account, so that the three records are aligned in real time.

A 0_+ and a 2_- whistler (see schematic diagram of Figures 3*a* and *c*) are also seen on the OGO 1 record of Figure 8*b*. Their lightning source is shown on the ELT record by the vertical line near 2.2 sec. This line is broken to indicate the excess propagation time of the lightning impulse to Stanford. The same lightning impulse also produced a multicomponent one-hop whistler at SES, top record. Although the 2_- whistler presents a fairly well-defined trace at the approximate position of the arrow, it is preceded by some smeared components. These components are consistent with coupling between lower L-value ducts observed later and the duct being directly observed by the satellite. The sources of the 0_+ whistlers as observed at the USNS Eltanin were generally somewhat poorer in quality than the sources of the 1_- whistlers observed at SES. This may have resulted because the Eltanin was nearly 3500 km from the southern foot of the field line passing through the satellite, while SES was only about 1500 km from the northern foot.

Figure 9 is similar to Figure 8 but corresponds to data recorded about a minute later, when the satellite was inside a different duct. Careful examination of the spectra of the 1_- whistlers from both figures reveals that their shapes and travel times are different. The corresponding shapes are drawn enlarged in Figure 10 (ducts 2 and 3, respectively).

Test of the ducted nature of the whistlers of

October 20, 1964. To verify the ducted nature of the events just described, the four tests indicated above may be applied as follows:

(1) The frequency-time spectra of the observed 0_+ and 1_- components agree closely with the shapes predicted by the longitudinal approximation. The frequency of minimum travel time (nose frequency) of the 1_- whistler is within 7% of the value calculated by assuming longitudinal propagation and the Jensen and Cain field. This discrepancy, although significant, is not enough to disqualify such whistlers as ducted, because ray tracing in a smooth magnetosphere without field-aligned enhancements of ionization shows that the nose frequency of the nonducted 1_- whistler that reaches the satellite is less than half the nose frequency of the ducted 1_- whistler. This point will be discussed further in a later section.

(2) The ratio of the observed travel time of the 1_- whistler to that of the 0_+ whistler is within 15% of the value predicted by the longitudinal approximation using the Jensen and Cain field. As in the case of the nose frequency, this level of agreement is regarded as satisfactory, and the discrepancy will be discussed in a later section.

(3) In Figure 8*b*, the difference between the travel time of the best defined component of the 2_- whistler and the 0_+ whistler is equal to twice the travel time of the 1_- whistler of the same record (within 2%). This simple time relationship holds for the entire frequency range in which the whistlers are well-defined and indicates that a single path is followed back and forth. Such behavior is clearly not exhibited by the nonducted whistlers of Figures 1 or 5. Incidently, the travel time of the leading component of the 2_- whistler of Figure 8*b* is consistent with one-hop northward propagation along duct number 6 (Figure 10), reflection at the base of the ionosphere, and propagation to the satellite along duct number 2.

(4) The spectra of successive 1_- whistlers were compared (especially for nose frequency and travel time at the nose), and only five discrete changes were observed. Other than the discrete variations, all of the 1_- components have indistinguishable shapes and travel times. (Compare 1_- whistlers in each of Figures 8*b* or 9*b*.) The six distinct spectra observed are sketched in Figure 10, which was obtained by tracing the actual spectra from enlarged copies of the records. The region within which the satellite receives 1_- whistlers with the same spectral shape and travel time is identified as a duct. This behavior is not exhibited by the sequence of nonducted (MR) whistlers of Figure 4, in which the components of successive whistlers were found to be different, indicating the existence of a continuum of whistler paths, rather than a set of discrete ones.

On the basis of the four tests performed, it is concluded that the OGO 1 whistlers described reached the satellite via field-aligned ducts.

6. Properties of the Magnetosphere Deduced from Ducted Whistlers

Whistler ducts. If the spacing in time between successive observations of ducted whistlers is sufficiently small, the effective duct dimensions and separations can be determined from in situ measurements. This is done by assuming that a duct covers just the region of space where whistler components having the same spectral shape are observed. As an example, the extent of ducts number 2 or number 3 (in which the whistlers of Figures 8*b* and 9*b*, respectively, where observed) along the OGO 1

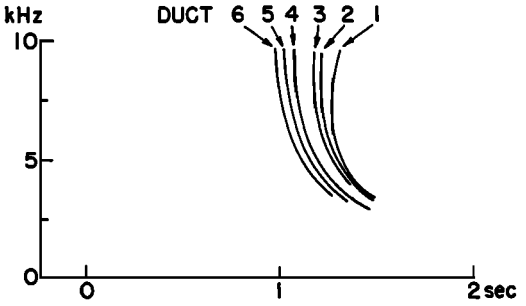

Fig. 10. Tracings of the frequency-time spectra of the 1_- ducted whistlers received at OGO 1 on October 20, 1964, from 0921 to 0933 UT. The abscissa origin marks the time of the causative atmospheric, which was identified in ground records from SES (see Figures 8 and 9). While the satellite was inside a duct, the same spectral shape was observed. Discrete changes in time delay and nose frequency took place when the satellite moved from one duct to the next. Six ducts were observed. Ducts number 2 and number 3 correspond to the data shown in Figures 8*b* and 9*b*, respectively.

orbit is ~500 km, corresponding to an L-shell thickness of ~0.06 R_E or a 60-km extent in latitude at an altitude of 1000 km. The effective separation between these two ducts, identified by the interval between successive 1₋ whistlers with different shapes and travel times, was found to be only about 55 km along the OGO 1 orbit, corresponding to a 7-km separation in latitude at an altitude of 1000 km.

In the present study, the 0₊ whistlers were not useful in duct identification for several reasons. The nose frequency was above the receiver upper cutoff of 12.5 khz, and changes in spectral shape were difficult to observe. Also, the travel times were small, so that the error in alignment of the records (the largest source of error in travel time) frustrated attempts to detect discrete travel-time changes.

The uncertainty in travel time would be virtually eliminated if telemetry from a southern hemisphere station were available, and if VLF data received on the ground had been recorded on the same magnetic tape with the satellite data. Owing to these limitations, it is not possible to distinguish a ducted from a nonducted 0₊ whistler in the records. On the other hand, the corresponding ducted and nonducted 1₋ whistlers are readily distinguishable, since their nose frequencies differ by a factor of at least 2.

Results on the field line distribution of thermal ionization. Ducted whistlers observed in the magnetosphere provide a unique means of testing various models of the distribution of thermal ionization along the field lines. One test involves assuming a field line model and obtaining separate estimates of the equatorial electron concentration from the travel times of the 0₊ and 1₋ whistlers, respectively. The smallness of the disparity between the estimates is a test of the applicability of the model used in the calculations. Another method is to compare observed and calculated nose frequencies of 0₊ and 1₋ whistlers using various models of the field-line distribution in the calculations.

Two field-line models were tested with the ducted whistlers described above, a diffusive-equilibrium (DE) model [see *Angerami and Thomas*, 1964 or *Angerami*, 1966] and the more rapidly varying $N \propto R^{-4}$ model (approximately a gyrofrequency model). Empirical support for the diffusive-equilibrium model has previously been obtained using ground whistler data and Alouette 1 densities at 1000 km [*Angerami*, 1966; *Angerami and Carpenter*, 1966]. The equatorial electron concentrations calculated for each of six ducts are illustrated in Figure 11, where the filled triangles and circles indicate the numbers obtained using the DE model, and the unfilled triangles and circles indicate the sample values obtained using the R^{-4} distribution. The values obtained from 0₊ and 1₋ events using the DE model agree within 30%, while for R^{-4} there is a difference by roughly a factor of 2.5.

Also plotted in Figure 11 are equatorial densities (square symbols) determined from two nose whistlers received at SES (similar to but better defined than the one-hop whistlers of Figure 8). Although these densities are not directly comparable to the satellite measurements, due to a probable difference in path longitude of about 30°, it appears that the DE model provides much better agreement not only among the various satellite measurements but between the ground and satellite data as well.

The nose frequency test was also applied to the two models, and again the agreement between the observations and the DE model was

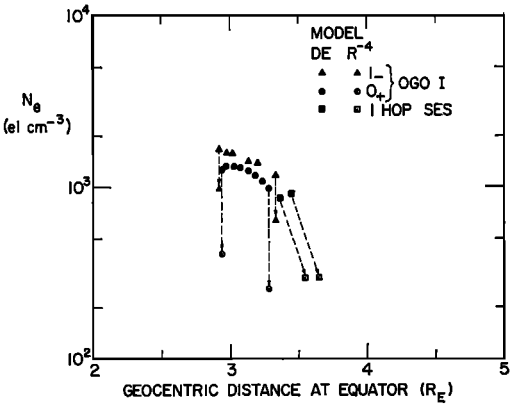

Fig. 11. Equatorial electron concentrations derived from whistler observations. A reasonable agreement exists between the densities derived from the 0₊, 1₋, and one-hop whistlers when a diffusive equilibrium (DE) model is used in the analysis (filled symbols). On the other hand, the use of the R^{-4} model leads to large discrepancies (open symbols), indicating that the DE model is a much better approximation to the actual field-line distribution of ionization.

much better, involving a disparity of only 7% as opposed to 22% for the R^{-4} case.

Discussion of discrepancies between calculated and observed parameters of ducted whistlers. A close comparison between calculated whistler parameters and the events observed on October 20, 1964, revealed small but significant discrepancies:

(1) The measured nose frequencies of the 1₋ whistlers were lower (by about 7%) than the nose frequencies calculated.

(2) The 1₋ whistlers exhibited a greater travel time than was predicted by the calculations. At 5 khz the excess travel time is about 15%, resulting in electron concentrations calculated using the 1₋ data that are about 30% higher than those calculated using the 0₊ properties, as shown in Figure 11.

The calculations were performed using the longitudinal approximation for whistler propagation and the Jensen and Cain expansion for the earth's magnetic field. The density of ionization was assumed to follow a diffusive equilibrium (DE) model along the field lines, with a temperature of 1600°K and relative abundances of H^+, He^+, and O^+ at 1000 km equal to 0.02, 0.50, and 0.48, respectively. Wide variations in the relative composition did not appreciably change the results.

The uncertainties in measurement of travel time were less than 4%, and the uncertainties of nose frequency less than 3%; therefore other explanations of the discrepancies must be sought.

The possibility of failure of the longitudinal approximation was ruled out on the basis of OGO 3 data recently analyzed [*Smith and Angerami*, 1967]. Using the actual local magnetic field measured from the Rubidium vapor magnetometer on OGO 3, the agreement between nose frequencies of 0₊ whistlers observed and calculated was found to be within the measurement uncertainty of 3%. A correspondingly precise test of the longitudinal approximation would not be possible with 1₋ whistlers. Recall that in the longitudinal approximation the nose frequency of a whistler is in general strongly dependent on the minimum gyrofrequency along the path traversed. For a 0₊ whistler this minimum gyrofrequency occurs at the satellite, and the knowledge of the geomagnetic field intensity at the spacecraft defines the nose frequency with small uncertainty due to changes in other parameters. The same is not true for a 1₋ whistler, because it travels through regions of lower magnetic field intensity and thus has a nose frequency sensitive to the geometry of the magnetic field beyond the satellite.

A change in the field-line model of ionization distribution to remove the discrepancies must be such as to place relatively more ionization near the top of the field line. This would tend to lower the nose frequency [cf. *Angerami*, 1966] and to increase the time delay of the 1₋ whistler. Reasonable changes of model were tried unsuccessfully; significant discrepancies remain even with the use of a constant density model.

The time delay discrepancy could be removed by assuming asymmetrical ionization, such that the density in the northern part of the field line (see Figure 3*a*) is about 30% higher than in the southern part, but this hypothesis is considered unlikely because the predictions for f_0F_2 indicate much higher values in the southern foot of the field line through the satellite. In any case, the nose frequency discrepancy would not be removed.

Uncertainty in the satellite position might possibly explain the discrepancies. For example, a 2° southward displacement from the reported position, with altitude unchanged, allows calculations and measurements of both nose frequencies and travel times to be simultaneously reconciled. This possible explanation remains to be fully appraised.

The possibility of a distortion in the field line with respect to the assumed Jensen and Cain field remains to be explored. It is necessary that the minimum magnetic field intensity along the line of force passing through the satellite be about 7% smaller than that given by the Jensen and Cain model. At the same time, the portion of the line of force (Figure 3*a*) extending from the satellite across the equator to a northern foot should be about 12% longer than that calculated by the Jensen and Cain model. Two possible distortions are considered.

The first is an inflation of the magnetosphere by a ring current. The magnetic activity index *Kp* was equal to 3 at the time of the observation, but a medium severe storm (*Kp* =

5 for 6 hours) occurred in the preceding day [*Lincoln*, 1965]. In the recovery phase of more severe storms, *Cahill* [1966] reported ring current effects as close to the earth as $L = 3$. The distortions reported amounted to changes in direction of the field by $\sim 15°$, and depressions in magnitude by $\sim 40\ \gamma$. There is also evidence of some inflation of the field at quiet times beyond 3.5 R_E, with observed field direction changes by as much as 20 or 30° [*Mead and Cahill*, 1967].

Another possibility is an asymmetrical distortion in the field, due to oblique incidence of the solar wind upon the dipole field. At the time of the observations, the earth-sun line was about 16° south of the dipole equator. It might be expected that the magnetic field near OGO 1 on the nightside would be blown slightly northward, causing the 1_ path of Figure 3*a* to be extended and to reach regions of lower field intensities. The geometry of the asymmetrical distortion is more convenient to the explanation of the whistler data presented here than is the symmetrical inflation, in that it requires smaller changes in field direction. There is some evidence for asymmetrical distortions in the magnetic field, both under conditions of oblique and normal incidence of the solar wind [*Little et al.*, 1965; *Mead and Cahill*, 1967].

The explanation of the data by field distortions remains among the possibilities to be appraised. Some numerical calculations using the asymmetrical distortion were attempted but were unsuccessful, probably owing to an inadequate model of the cavity field for the case of oblique incidence of the solar wind. The amount of distortion needed was estimated by a crude calculation in which the direction of the field was supposed different from the dipole field at each point, by a constant angle. It was estimated that an angle of 6–8° would be sufficient to explain the whistler data.

7. Regions of Observation and Relative Frequency of Occurrence of Various Types of Whistlers

Most ducted whistlers are observed at magnetic shells beyond $L \sim 2.5$, corresponding to the magnetospheric region of propagation of most whistlers received on the ground. Whistlers classified as magnetospherically reflected (MR) are commonly observed at L shells of 1.5–3, and at magnetic latitudes less than 30°.

The most frequently observed type of whistler exhibits several components and includes both nonducted and either ducted or 'mixed-path' cases. The mixed-path whistlers are events for which part of the propagation path appears to be ducted and part nonducted. Details of such events remain to be described. Less commonly observed are whistlers of the MR type only. Even less common are purely ducted events.

8. Conclusions

Nonducted propagation. A new type of nonducted, echoing whistler has been detected at low latitudes in the magnetosphere in the range $L = 1.5$–3. This event, the magnetospherically reflected or MR whistler, has been qualitatively explained in terms of *Kimura's* [1966] ray tracing. The path involves reflections of the energy back and forth across the magnetic equator. The turning points involve: a frequency limitation imposed by the local lower hybrid resonance frequency and a refraction of the wave normal through 90°, due to the presence of ions, as in the case for the subprotonospheric whistler.

Another new phenomenon reported here is the 'Nu' whistler, a particular case of the MR event. The lowest observed frequency at which the two traces of the Nu whistler join is a lower limit for the lower hybrid resonance frequency at the satellite, a result that may offer possibilities for study of properties of the medium.

With the aid of *Kimura's* [1966] ray tracing in a smooth magnetosphere in which the electron concentration along the field lines follows a diffusive equilibrium distribution it has been possble to explain the main features of MR and Nu whistlers. These phenomena provide therefore experimental support for the validity of Kimura's ray tracing results and the diffusive equilibrium model.

Many detailed features of the MR whistler remain to be fully described and explained. Some of the irregular features of the traces may eventually be attributed to the presence of irregularities in an otherwise smooth medium.

The findings of the present research are consistent with the general theoretical predictions

TABLE 2. Characteristics of Whistler-Mode Propagation in the Magnetosphere

Ducted	*Nonducted*
(1) Signals observed on the ground	Signals *not* observed on the ground
(2) Propatation at small wave normal angles	Propagation at *large* wave normal angles
(3) Path independent of initial wave normal or frequency	Paths dependent on wave as well as medium properties
(4) Discrete paths not yet predictable (depend on existence of ducts)	Topological continuum of paths, which are predictable to first order
(5) Field-aligned irregularities play decisive role	Ions play decisive role (in MR's)

for nonducted propagation in the magnetosphere listed in Table 2.

Ducted propagation. The first direct evidence of 'whistler ducts' in the magnetosphere has been obtained through analysis of the dispersion properties of a set of 0_+ and 1_- whistlers recorded on OGO 1. The ducted nature of the whistlers was verified by self-consistency tests among several components, including evidence of discrete changes in dispersion properties as the satellite moved from one duct to another. In general the findings are consistent with the theoretical predictions for ducted propagation listed in Table 2.

Properties of the magnetosphere. The analysis of ducted whistlers provided strong support for the diffusive equilibrium type of distribution of ionization along the field lines in the plasmasphere. The analysis also provided the first local measurement of whistler duct sizes in the plasmasphere, these being about 0.06 in L value, or about 400 km at the equator at $L \sim 3$. The spacings between the observed ducts ranged from 50 to 500 km measured radially at the equator near 3 R_E.

From the study of small discrepancies between the calculated and observed parameters of ducted whistlers, it appears that if the position of the satellite is accurately known within, say 50 km, it should be possible to detect certain types of distortions of the geomagnetic field line passing through the satellite. This would be done by comparison of the travel time of 0_+ and 1_- ducted whistlers and by measurement of the spectral shape of the latter.

9. Suggested Technical Features of Future Experiments

The usefulness of the data reported here was enhanced by the following technical features:

(1) Broadband (0.3–12.5 khz) VLF data from OGO 1, which was telemetered to ground stations in real time in a low interference FM channel.

(2) Simultaneous broadband VLF recordings from whistler stations situated in opposite hemispheres and near the meridian of the satellite.

(3) Precise timing (within approximately 10 msec) on all simultaneous records.

Any significant degradation in the quality of data, either in interference, data rate, or timing, would probably obscure the effects that lead to many of the conclusions of this paper. It is therefore suggested that further VLF work in

Fig. 1. *Smith and Angerami.* A magnetospherically reflected (MR) whistler. The satellite is at 5.9°S geomagnetic latitude, $L = 2.4$, altitude = 8749 km. Local time is 0520. The dark trace at about 7 khz is interference associated with a voltage-controlled oscillator used to indicate amplitudes. The approximate time of the causative atmospheric is denoted by the arrow (see text). Each whistler component is labeled according to the notation of Figure 2 (see also Figure 4). The AGC effect of the log-compressor is apparent through the suppression of the background noise by the whistlers. Three components of a second event are shown near the end of the record.

Fig. 5. *Smith and Angerami.* Time-frequency spectra of MR whistlers observed on OGO 1 at different geomagnetic latitudes. The time and position of the satellite is shown above each record. The approximate time of each source is indicated by an arrow. Note the change of spacing of the traces as a function of geomagnetic latitude. Compare the spectra in (*a*) and (*f*) to the sketches of Figures 4*b* and *d*, respectively.

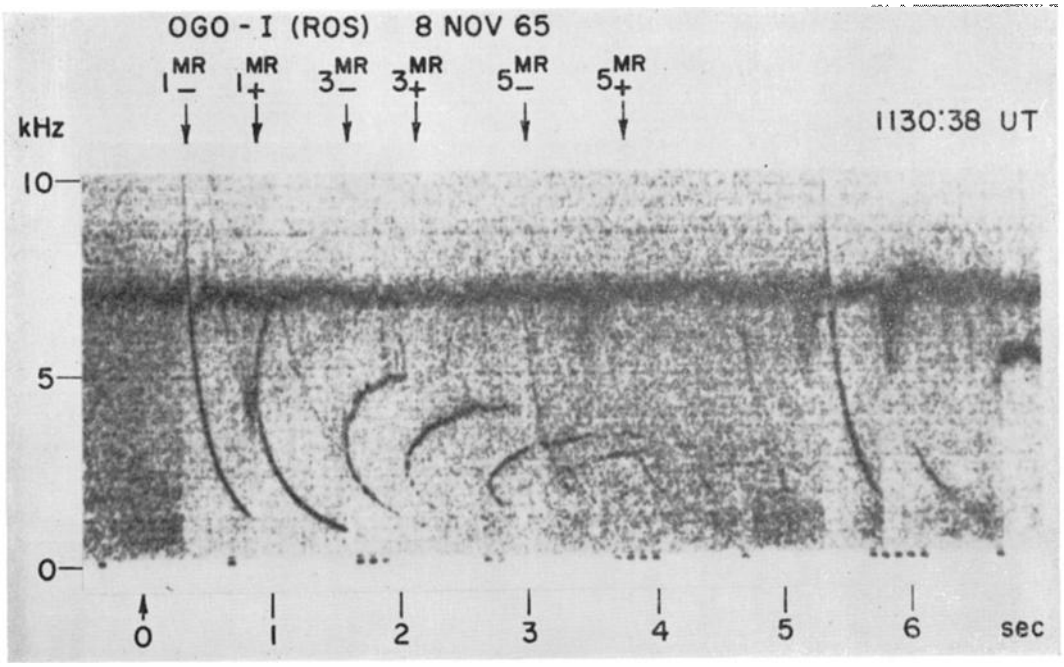
OGO - I (ROS) 8 NOV 65
1 MR −
1 MR +
3 MR −
3 MR +
5 MR −
5 MR +
kHz
1130:38 UT
10
5
0
0
1
2
3
4
5
6
sec

Fig. 1.

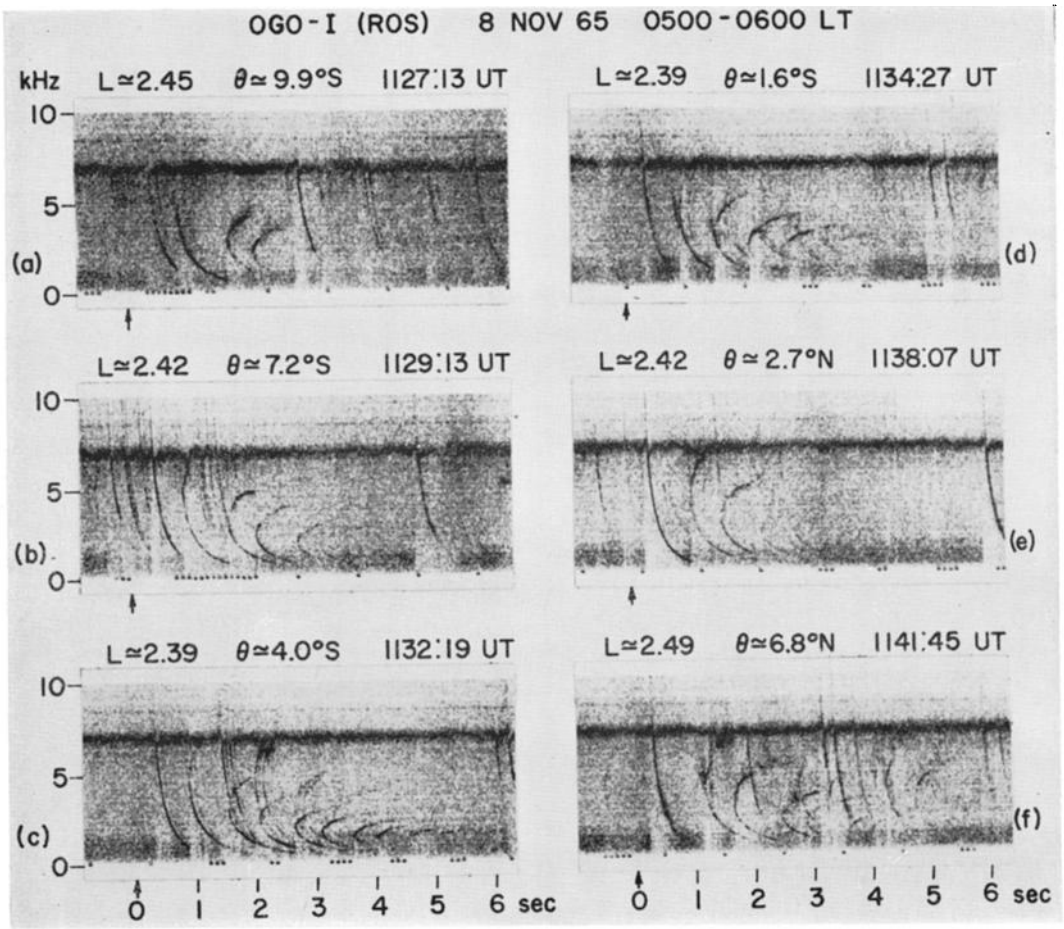
OGO - I (ROS) 8 NOV 65 0500 - 0600 LT
kHz
L≃2.45 θ≃9.9°S 1127:13 UT
L≃2.39 θ≃1.6°S 1134:27 UT
(a)
(d)
L≃2.42 θ≃7.2°S 1129:13 UT
L≃2.42 θ≃2.7°N 1138:07 UT
(b)
(e)
L≃2.39 θ≃4.0°S 1132:19 UT
L≃2.49 θ≃6.8°N 1141:45 UT
(c)
(f)
10
5
0
0 1 2 3 4 5 6 sec

Fig 5.

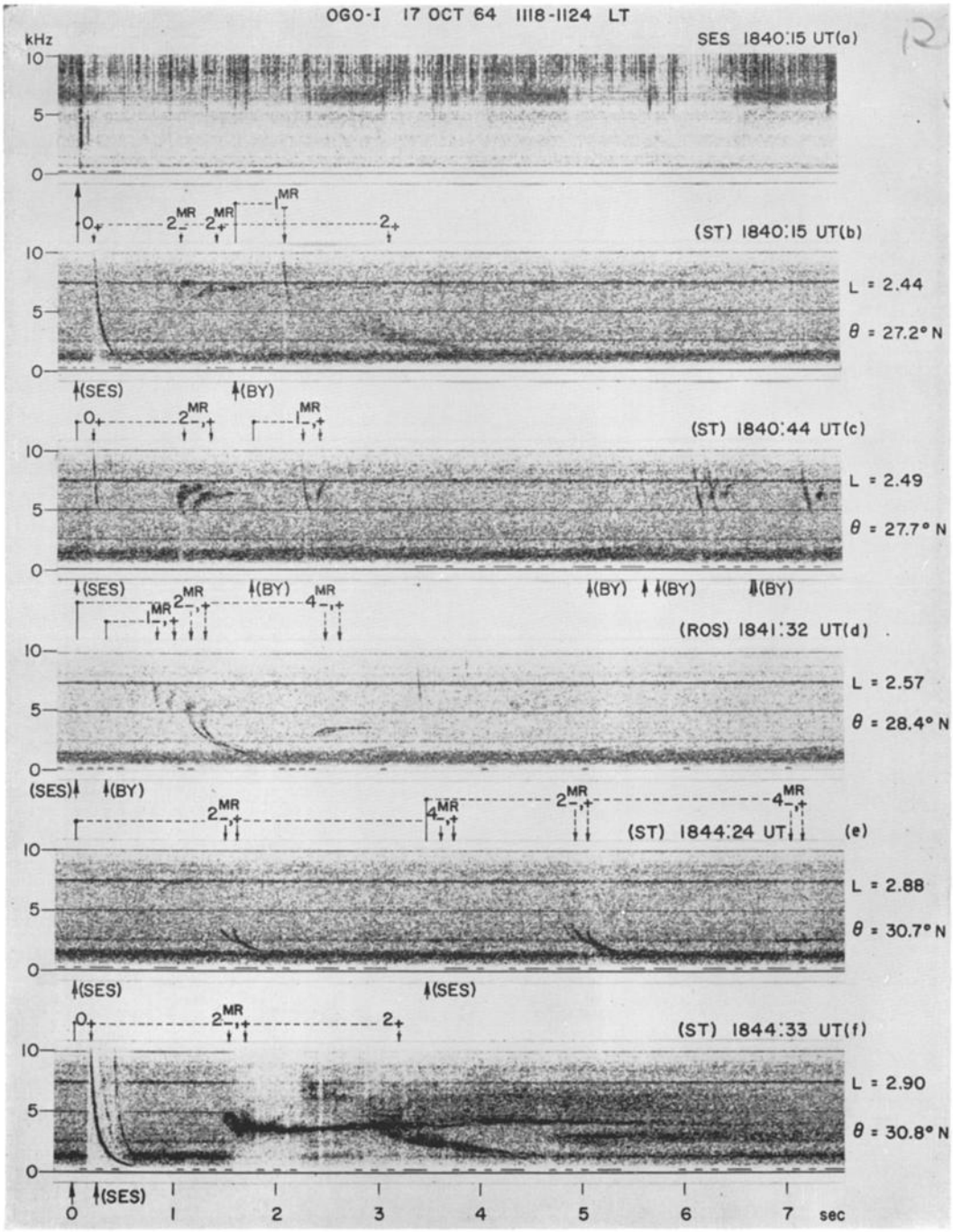

Fig. 6. *Smith and Angerami.* MR whistlers, Nu whistlers, and MR excitation of emissions as observed on October 17, 1964. For comparison, panel (*a*) shows spectra of data from the SES ground station corresponding to the OGO 1 data of panel (*b*). Panels (*b*) through (*f*) are samples of spectra of VLF data collected on an outbound pass of OGO 1. The telemetry stations are indicated in parenthesis in the top of each record (see Table 1). The horizontal lines at 2.461 khz and harmonics are interference lines from the satellite DC to DC power converter. The times of sources of most of the whistlers are indicated by the arrows.

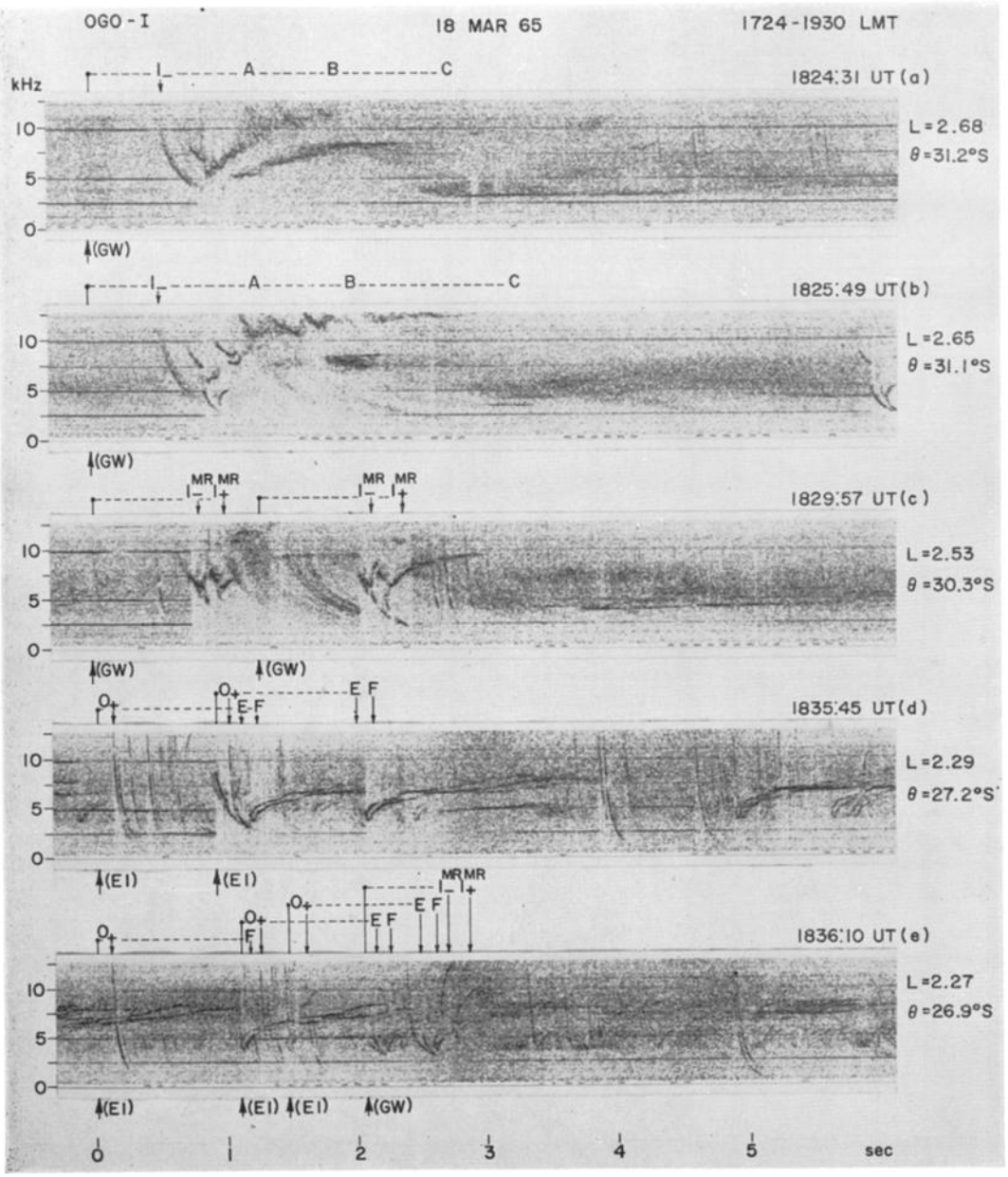

Fig. 7. *Smith and Angerami.* Unusual whistlers from OGO 1. The arrows below each spectrogram indicate the time of origin of atmospherics that are related to the traces as indicated by the lines above each figure. The indicated time above each figure gives the time (to the nearest second) of the leftmost arrow at the bottom of the respective figure. The time scale indicates time in seconds past this mark.

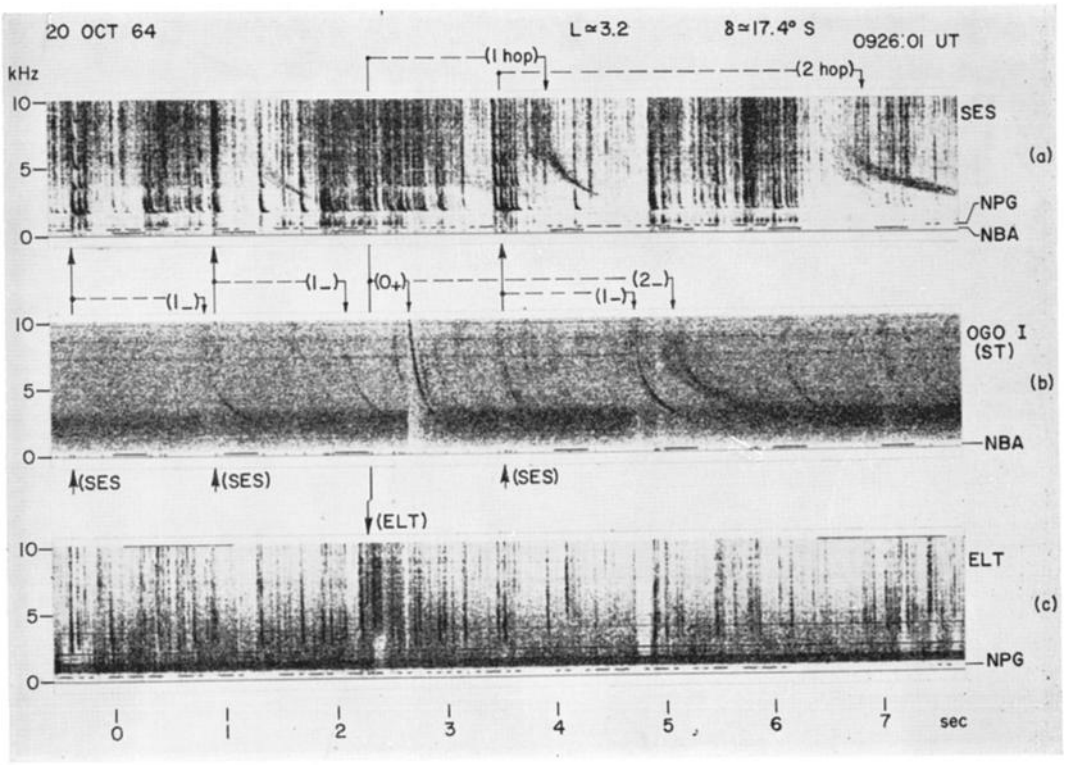
20 OCT 64
L≃3.2
δ≃17.4° S
0926:01 UT
kHz
(1 hop)
(2 hop)
SES
(a)
NPG
NBA
(1_)
(1_)
(0+)
(2_)
(1_)
OGO I
(ST)
(b)
NBA
(SES
(SES)
(SES)
(ELT)
ELT
(c)
NPG
0
1
2
3
4
5
6
7
sec

Fig. 8.

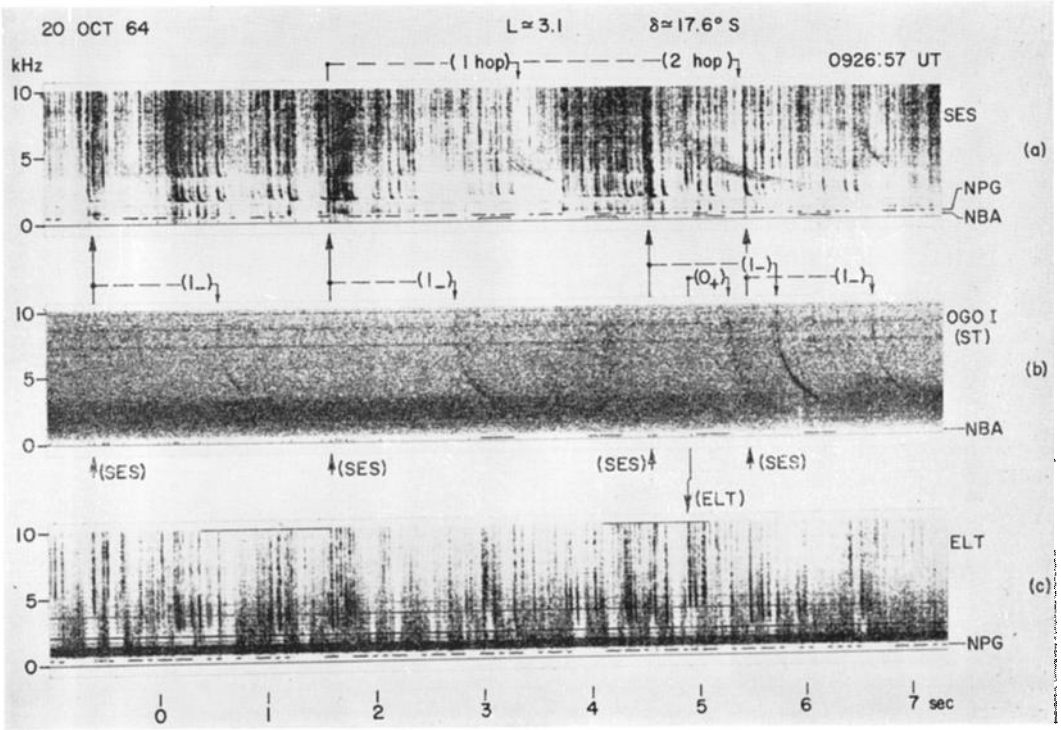
20 OCT 64
L≃3.1
δ≃17.6° S
0926:57 UT
kHz
(1 hop)
(2 hop)
SES
(a)
NPG
NBA
(1_)
(1_)
(0+)
(1_)
(1_)
OGO I
(ST)
(b)
NBA
(SES)
(SES)
(SES)
(SES)
(ELT)
ELT
(c)
NPG
0
1
2
3
4
5
6
7 sec

Fig. 9.

satellites continue to use high-capacity telemetry channels with data rate at least equal to that yielded by the special purpose channel presently used in OGO 1. This is an FM channel that transmits in real time a broadband of 0.3–12.5 khz with a dynamic range of 20 db. Furthermore, it is proposed that broadband VLF receivers be installed at the stations of the telemetry network, so that VLF ground data be recorded on the same magnetic tape as the satellite data. This procedure will increase many times the amount of VLF data from satellites that are suitable for detailed study. In addition, the analysis will be much easier and more accurate, owing to the absence of alignment errors.

Acknowledgments. We thank the many workers on the OGO project at the National Aeronautics and Space Administration and at TRW Systems for contributing to the success of the Stanford University/Stanford Research Institute OGO 1 VLF experiment. Our work was carried out under the leadership of R. A. Helliwell, the principal investigator. L. H. Rorden designed the experiment package and supervised its construction. John Katsufrakis coordinated the collection and reduction of the data used in this paper and brought important data to the attention of the authors. We are grateful to D. L. Carpenter for many helpful comments on this paper.

This research was supported in part by the National Aeronautics and Space Administration under contract NAS 5-2131, and in part by the Atmospheric Sciences Section of the National Science Foundation under grant GA-775. The ground VLF data were acquired under grants from the Atmospheric Sciences Section and the Office of Antarctic Programs of the National Science Foundation.

References

Angerami, J. J., A whistler study of the distribution of thermal electrons in the magnetosphere, *SEL-66-017, Radioscience Lab., Stanford Electronics Labs, Stanford University, Stanford, California,* May 1966.

Angerami, J. J., and D. L. Carpenter, Whistler studies of the plasmapause in the magnetosphere, 2, Electron density and total tube content near the knee in magnetospheric ionization, *J. Geophys. Res., 71,* 711, 1966.

Angerami, J. J., and J. O. Thomas, Studies of planetary atmospheres, 1, The distribution of electrons and ions in the earth's exosphere, *J. Geophys. Res., 69,* 4537, 1964.

Barrington, R. E., and J. S. Belrose, Preliminary results from the very low frequency receiver aboard Canada's Alouette satellite, *Nature, 188,* 651, 1963.

Brice, N. M., and R. L. Smith, Lower hybrid resonance emissions, *J. Geophys. Res., 70,* 71, 1965.

Cahill, L. J., Jr., Inflation of the inner magnetosphere during a magnetic storm, *J. Geophys. Res., 71,* 4505, 1966.

Carpenter, D. L., N. Dunckel, and J. F. Walkup, A new very low frequency phenomenon: whistlers trapped below the protonosphere, *J. Geophys. Res., 69,* 5009, 1964.

Cartwright, D. G., Rocket observations of very low frequency radio noise at night, *Planetary Space Sci., 12,* 11, 1964*a*.

Cartwright, D. G., Rocket observations of the intensity of very low frequency noise above the ionosphere, *Planetary Space Sci., 12,* 751, 1964*b*.

Edgar, B. C., and R. L. Smith, Magnetospherically reflected whistlers in OGO 1, paper presented Fall URSI Meeting, Palo Alto, California, December 1966.

Helliwell, R. A., *Whistlers and Related Ionospheric Phenomena,* Stanford Press, Stanford, California, 1965.

Jensen, D. C., and J. C. Cain, An interim geomagnetic field, (abstract), *J. Geophys. Res., 67,* 3568, 1962.

Kimura, I., Effects of ions on whistler-mode ray tracing, *Radio Sci., 1* (New Series), 269, 1966.

Lincoln, J. Virginia, Geomagnetic and solar data, *J. Geophys. Res., 70,* 2233, 1965.

Fig. 8. *Smith and Angerami.* Spectrograms of VLF signals simultaneously received at OGO 1 (center record, panel *b*) and at ground stations in opposite hemispheres. The code and second marks near zero frequency are translations of transmissions from NPG (18.6 khz) and NBA (18.0 khz), respectively, as received on the ground. Parts of the sferics are seen in the center record as dots at the NBA frequency. The relationship between a source and the corresponding whistlers is indicated by dashed horizontal lines. The sources of the 1_- whistlers are shown in SES by arrows. The sferic in ELT at ~2.2 sec produces 0_+ and 2_- whistlers in OGO 1 and one-hop whistlers in SES.

Fig. 9. *Smith and Angerami.* Similar to Figure 8, but recorded about one minute later, when the satellite had gone out of duct number 2 and into duct number 3. The time axis represents seconds after 09h 26m 57s UT. The sources of the 1_- whistlers are indicated by arrows in the SES record. The second of these also excites hybrid one-hop and two-hop whistlers, seen at SES. A somewhat diffuse 0_+ whistler and its source (in ELT) are shown near the 5-second mark.

Little, C. G., E. R. Schiffmacher, H. J. A. Chivers, and K. W. Sullivan, Cosmic noise absorption events at geomagnetically conjugate stations, *J. Geophys. Res., 70,* 639, 1965.

Mead, G. D., and L. J. Cahill, Jr., Explorer 12 measurements of the distortion of the geomagnetic field by the solar wind, *J. Geophys. Res., 72,* 2737, 1967.

Rorden, L. H., L. E. Orsak, B. P. Ficklin, and R. H. Stehle, Instruments for the Stanford University/Stanford Research Institute VLF experiment (4917) on the EOGO satellite, *Stanford Res. Inst. Instr. Rept.,* Menlo Park, California, May 1966.

Smith, R. L., Propagation characteristics of whistlers trapped in field-aligned columns of enhanced ionization, *J. Geophys. Res., 66,* 3699, 1961.

Smith, R. L., An explanation of subprotonospheric whistlers, *J. Geophys. Res., 69,* 5019, 1964.

Smith, R. L., and J. J. Angerami, Whistler propagation in magnetospheric ducts, paper presented at the Conjugate Point Symposium, Boulder, Colorado, vol. 2, *Tech. Memo. IERTM-ITSA, 72,* July 1967.

Smith, R. L., and N. M. Brice, Propagation in multicomponent plasmas, *J. Geophys. Res., 69,* 5029, 1964.

Storey, L. R. O., An investigation of whistling atmospherics, Ph.D. dissertation, Cambridge University, Cambridge, England, 1953.

Yabroff, I., Computation of whistler ray paths, *J. Res. NBS-D, Radio Propagation, 65,* 485, 1961.

(Received August 21, 1967.)